

Joint Learning of Instance and Semantic Segmentation for Robotic Pick-and-Place with Heavy Oclusions in Clutter

Kentaro Wada, Kei Okada and Masayuki Inaba
University of Tokyo, JSK Laboratory
{wada, k-okada, inaba}@jsk.imi.i.u-tokyo.ac.jp

Abstract— We present joint learning of instance and semantic segmentation for visible and occluded region masks. Sharing the feature extractor with instance occlusion segmentation, we introduce semantic occlusion segmentation into the instance segmentation model. This joint learning fuses the instance- and image-level reasoning of the mask prediction on the different segmentation tasks, which was missing in the previous work of learning instance segmentation only (instance-only). In the experiments, we evaluated the proposed joint learning comparing the instance-only learning on the test dataset. We also applied the joint learning model to 2 different types of robotic pick-and-place tasks (random and target picking) and evaluated its effectiveness to achieve real-world robotic tasks.

I. INTRODUCTION

Recently, with the help of deep convolutional networks, the vision community has been rapidly improved the performance of pixel-wise object segmentation with image: *semantic segmentation* (predicting class label for pixels) [1]–[3] and *instance segmentation* (predicting class label and pixel-wise mask for instances) [4]–[7]. However, these tasks have been tackled independently, and the effect of the joint learning and collaboration of both tasks is less explored.

For robotic manipulation, pixel-wise object segmentation is a crucial component. Previous work utilizes semantic segmentation models for pick-and-place of various objects [8]–[13]. Since semantic segmentation can not segment different instances in the same class, the work assumes that same class objects are not closely located and can be segmented by clustering.

Our previous work [14] applies instance segmentation model to instance-level picking task, in order to overcome that limitation. In addition to instance-level segmentation, we tackled occlusion segmentation of each instance (*instance occlusion segmentation*) in order to understand the stacking order of objects and decide the object picking order. In our previous work, we extended the state of the art model of instance segmentation [7], that firstly detects bounding boxes of object instance and then predicts pixel-wise mask of both visible and occluded regions inside each bounding box. Compared to instance segmentation, instance occlusion segmentation is still challenging because the model needs to predict bounding boxes of whole (visible + occluded) region and occluded region mask based on the whole shape estimation in each bounding box. Since mask prediction depends on the predicted boxes, the predicted mask in small boxes can be truncated.

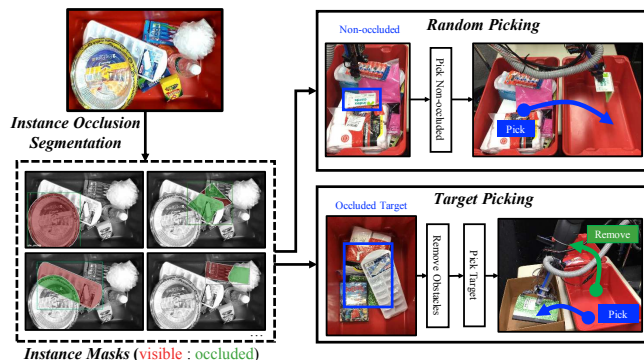


Fig. 1: Robotic pick-and-place based on instance occlusion segmentation. The instance occlusion segmentation model segments both visible and occluded regions of each object instance. This segmentation is helpful for different types of pick-and-place task: finding fully visible objects for *random picking*; and finding obstacle objects, which is occluding the target, for *target picking*.

Although instance occlusion segmentation is challenging, it is useful for robotic pick-and-place applications: random and target picking (Figure 1). For random picking in which there is no designated object, robot needs to find non-occluded (fully visible) objects to avoid grasp fail because of the collision to other objects. For target picking, robot needs to find heavily occluded target object and understand occlusion relationship among objects for planning of the appropriate grasp order to quickly remove obstacles and access the target. This consideration motivates us to improve instance occlusion segmentation models, to achieve robotic picking task with heavily occluded objects in clutter.

In this paper, we explore the collaboration of semantic and instance occlusion segmentation as shown in Figure 2. As noted before, the difficulty in instance occlusion segmentation is caused by the two-stage prediction: *image* \rightarrow *box* \rightarrow *mask*, especially wrong prediction of the whole bounding box in the 1st stage (*image* \rightarrow *box*). On the other hand, semantic occlusion segmentation is one-stage prediction of *mask* from *image*: *image* \rightarrow *mask*, though multiple instances in the same class are not discriminated. We anticipate that predicting whole bounding box in instance segmentation is difficult because there is no supervision of visible and occluded region at the 1st stage. This motivates us to jointly train bounding box prediction and mask prediction in the 1st stage by introducing semantic occlusion segmentation into the instance occlusion segmentation model.

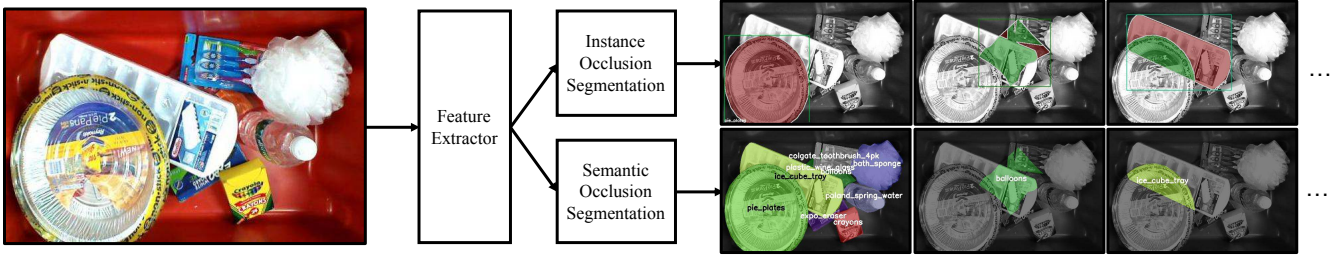


Fig. 2: Joint learning of instance and semantic occlusion segmentation.

In the experiments, we evaluated the proposed models trained with a dataset which contains scenes of various objects located in clutter. We also applied the joint learning model to real-world robotic picking task, and demonstrated its efficiency for both target picking (pick-and-place of designated objects) and random picking (pick-and-place of all objects) task in clutter.

In summary, our main contributions are:

- Occluded region segmentation learning with CNN-based pixel-wise score regression;
- Joint learning of instance and semantic segmentation for instance visible and occluded regions;
- Robotic target and random picking task achievement with heavy occlusions among objects.

II. RELATED WORK

A. Instance Visible and Occluded Region Segmentation

Instance segmentation is aimed at predicting object class and the pixel-wise mask of each instance in an image. In previous work, this task is mainly tackled in two different approaches: generate instance mask proposals and then classify [15, 16], detect instances with bounding box and then apply pixel-wise segmentation [4, 7]. Recently, Mask R-CNN [7], which uses the second approach is proposed as the state-of-the-art model of instance segmentation. This model extends the bounding box detection model, Faster R-CNN [17], to detect box and predict pixel-wise mask inside the box. Our previous work [14] extends Mask R-CNN for both visible and occluded region mask segmentation with pixel-wise prediction of multi-class instance masks (background, visible and occluded).

In this paper, we introduce joint learning of instance and semantic segmentation for visible and occluded regions. In the semantic segmentation part, we use a similar architecture as FCIS [4], which predicts position-sensitive masks (e.g., right-top of an instance) as a pixel-wise classification. In the instance segmentation part, we use the extended Mask R-CNN for multi-class instance masks. This joint learning introduces collaboration of different level of mask reasoning of instance segmentation (instance-level reasoning for instance mask prediction) and semantic segmentation (image-level reasoning for image pixel-wise class prediction), which is missing in the previous model.

B. Joint Learning

Joint learning of different vision tasks has been tackled in a lot of previous work. For example, Mousavian et al. [18]

propose jointly training semantic segmentation and depth estimation with pixel-wise score regression for image. Cheng et al. [19] propose joint learning of semantic segmentation and optical flow for video, and Baslamisli et al. [20] propose that of semantic segmentation and intrinsic image. The previous work trains pixel-wise score regression model (image-level reasoning) for different kinds of output labels (e.g., semantic labels + depth).

In the joint learning of instance and semantic segmentation, the model is trained for very similar outputs: object region masks. On the other hand, these outputs are predicted based on different kind of reasoning: image-level for semantic segmentation and instance-level for instance segmentation, which was missing in the previous work. Also, the joint learning in this paper does not require any additional labels annotated by human, since ground truth semantic segmentation masks can be generated by the masks of instance segmentation.

III. JOINT LEARNING OF INSTANCE AND SEMANTIC OCCLUSION SEGMENTATION

For collaboration of instance-level reasoning of instance segmentation and image-level reasoning of semantic segmentation, we train a neural network model for both tasks. As shown in Figure 2, the model shares feature extractor to learn commonly effective feature extraction for instance and semantic segmentation. In the following, we describe the detail of instance and semantic occlusion segmentation model for joint training.

A. Instance Occlusion Segmentation

As in our previous work [14], we extend an existing instance segmentation model, Mask R-CNN [7], for occlusion segmentation. The original Mask R-CNN is designed for segmenting only the visible regions of instances, so we extended the part of mask prediction for multi-class: visible, occluded and background as shown in Figure 3. The model firstly predicts bounding boxes of each instance and secondly predicts pixel-wise masks inside each box.

Pixel-wise prediction in the second stage is conducted by score regression with convolutional layers, and softmax cross entropy is computed as the loss (l_{mask}) for training. Other components are the same as the original Mask R-CNN:

- *Feature Extractor*: For the feature extraction from input image, we use ResNet50-C4 (C4 represents output of 4th layer of Residual Block) [21] pretrained on



(a) A scene.



(b) Visible. (c) Occluded. (d) Background.

Fig. 3: Multi-class masks of an object instance.

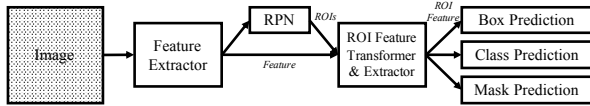


Fig. 4: Instance occlusion segmentation model.

large-scale image classification task, ImageNet [22] for weight initialization.

- **Region Proposal Networks (RPN):** It is firstly proposed in [17] for class-agnostic object bounding box prediction. It has two losses: bounding box regression (l_{box}^{rpn}) and classification for foreground and background (l_{cls}^{rpn}). The predicted bounding box is usually called ROI (region of interest) and used for the start point to predict refined class-specific box in the following components.
- **ROI Feature Transformer:** The extracted feature is transformed using the ROIs proposed by RPN. This normalizes the shape of the ROI which is important to apply instance-level reasoning to predict classes and refined bounding box regression by the following fully connected (FC) layers. ROIAlign [7] is an operation for ROI-based feature transformation, and it resizes the feature with bilinear interpolation.
- **ROI Feature Extractor:** 5th layer of ResNet50 (res5) is applied to extract ROI-based features after the ROI feature transform. The weight of res5 is also copied from pretrained model in ImageNet at initialization.
- **Classification and Class-specific Box Prediction:** These modules are firstly proposed in [23] for multi-class object bounding box detection, and both are predicted by FC layers from the transformed feature for ROIs. Similarly to region proposal networks, it has two losses: bounding box regression (l_{box}) and multi-class classification (l_{cls}).

To summarize, all components are connected as shown in Figure 4, and all losses are l_{box}^{rpn} , l_{cls}^{rpn} , l_{box} , l_{cls} and l_{mask} .



(a) Visible labels.



(b) Occluded masks.

Fig. 5: Semantic visible and occluded labels.

B. Semantic Occlusion Segmentation

For semantic (visible) segmentation, we extend previous work of semantic (visible) segmentation by fully convolutional networks (FCN) proposed in [1]. All layers are composed of convolutional or pooling layers, which keep the geometry of image, so FCN is known as effective and widely used for pixel-wise score regression tasks: depth prediction [24, 25], grasp affordance [12, 26, 27], optical flow [28], and instance masks [4, 6].

FCN for semantic segmentation is composed of feature extractor and pixel-wise classification. Original FCN [1] uses VGG16 [29] as the feature extractor, which is pretrained on image classification [22]. After the work of VGG, ResNet [21] has been proposed for image classification, and it showed better performance in image classification. Following the previous work [6], which uses ResNet-C4 and res5 as the feature extractor for pixel-wise score regression, we replace the VGG feature extractor with ResNet for better feature extraction and common feature extractor as instance segmentation in Figure 2.

For semantic segmentation task, pixel-wise classification module predicts n_{class} object scores for each pixel. n_{class} represents number of classes including *background* class that should be assigned to the other regions than the objects interest as shown in Figure 5a. If the input RGB image has size $(H, W, 3)$, the output scores has size (H, W, n_{class}) . For training, softmax cross entropy loss (l_{vis}^{sem}) is computed for the output scores, and at testing, the top-scored label is assigned for each pixel to get the visible label. In occlusion segmentation, however, there can be overlaps between the occluded regions of each class of objects. For example, in Figure 5b, the occluded region masks of *hanes_socks* and *laugh_out_loud_jokes* have overlap. Top-scored label assignment in semantic visible segmentation can not handle these cases.

To handle the overlap of occluded masks, we replace the loss of pixel-wise score regression from softmax cross entropy (class competitive) to sigmoid cross entropy (class

individual): l_{occ}^{sem} . With softmax cross entropy, the model tries to find most probable class for each pixel. On the other hand, with sigmoid cross entropy, the model tries to find the occluded probability for each pixel individually in all classes, which is suitable to occlusion segmentation. Since the occluded mask is only defined for foreground, the output size of FCN for occlusion segmentation is $(H, W, n_{class} - 1)$ (-1 represents the removal of background class).

All components are integrated as shown in Figure 6, and all losses in semantic occlusion segmentation are l_{vis}^{sem} and l_{occ}^{sem} .

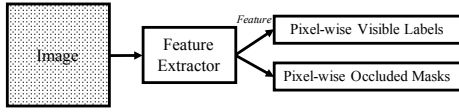


Fig. 6: Semantic occlusion segmentation model.

IV. JOINT TRAINING

A. Shared Feature Extractor

We jointly train fore-mentioned instance and semantic occlusion segmentation models. The feature extractor which is common in the model (Figure 2) is ResNet50-C4, and the weight of res5 is not shared. In instance segmentation model, res5 ($res5^{ins}$) extracts ROI features after ROI feature transformation from ResNet50-C4 features and ROIs. Since the ROI represents each instance in image, this feature extraction is specific for instance (instance reasoning). On the other hand, the res5 of semantic segmentation model ($res5^{sem}$) extracts features in image geometry without any information about instances.

B. Loss Balancing

As described above, losses for the instance occlusion segmentation are:

- l_{box}^{rpn} : for bounding box regression of region proposal networks (RPN);
- l_{cls}^{rpn} : for foreground vs background classification of RPN;
- l_{box}^{ins} : for instance bounding box regression;
- l_{cls}^{ins} : for instance classification;
- l_{mask}^{ins} : for instance visible, occluded and background masks.

And losses for the semantic occlusion segmentation are:

- l_{vis}^{sem} : for pixel-wise class visible score regression;
- l_{occ}^{sem} : for pixel-wise class occluded score regression.

For joint training of both tasks, we sum all losses and backward it:

$$l^{ins} = l_{box}^{rpn} + l_{cls}^{rpn} + l_{box}^{ins} + l_{cls}^{ins} \quad (1)$$

$$l^{sem} = l_{vis}^{sem} + l_{occ}^{sem} \quad (2)$$

$$l = l^{ins} + \lambda \cdot l^{sem}. \quad (3)$$

The λ represents the weight for loss balancing of instance and semantic occlusion segmentation. We show experimental results by changing that parameter in the following section.

V. EXPERIMENTS

A. Instance and Semantic Occlusion Segmentation

1) *Dataset for Evaluation*: We used 40 objects used in Amazon Robotics Challenge (ARC2017) following our previous work [14] (Figure 7). For training and evaluation, we collected image frames of cluttered scene, in addition to the dataset used in [14].



Fig. 7: Objects used in the experiments.

For more efficient data collection and annotation, we used following annotation process:

- 1) Fixed camera collects video frames of picking fully visible objects in cluttered scene by human.
- 2) Human annotates the fully visible objects in the video at the frame where it is picked (Figure 8).
- 3) Backproject the annotated mask to previous video frames to get visible and occluded masks assuming object is fixed in all frames.

With above rules, human only needs to annotate polygon only once per each instance. We created 51 videos (train:test = 33:18) in addition to 22 videos (14:8) in [14]. In total, there were 505 images (325:180). The created pair of input and output are as shown in Figure 2, with converting instance-level masks to class-level masks.

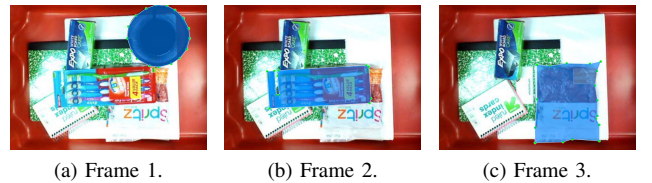


Fig. 8: Annotation process in a video.

2) *Evaluation Metric*: We jointly trained instance and semantic occlusion segmentation, but the objective is improving the result of instance occlusion segmentation, and achieving robotic picking task in scenes with heavily occluded objects. For the evaluation, we used the metric of instance occlusion segmentation to compare the baseline models proposed in our previous work [14], which is an extension of joint evaluation of detection and segmentation: PQ = Panoptic Quality [30]. Note that PQ is computed for each object class and then averaged to get the metric for multi-class instance segmentation. It is represented as mPQ (mean of PQ).

TABLE I: Results of joint/non-joint learning.

model	λ	mPQ
instance-only	-	41.0
	1	40.9
	0.5	41.7
joint (instance + semantic)	0.25	42.2
	0.1	41.8

3) *Data Augmentation*: Since objects' cluttered scene has a large number of variations even with a fixed number of objects, data augmentation is important for robust prediction with the new images in the test dataset. We applied following augmentations:

- HSV color: for the change of brightness and the color of objects;
- Gaussian blur: for blur in frame by camera movement;
- Affine transform: for the scale, rotation, translation, and shear change.

The HSV color and Gaussian blur augmentation are applied to the RGB image of camera, and affine transform is applied for both RGB and instance mask annotations. The sample result of above augmentations is shown in Figure 9.

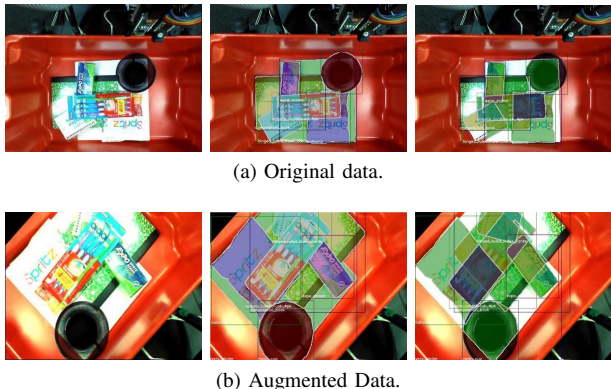


Fig. 9: Data augmentation. RGB image (right), instance visible (center) and occluded (right) masks.

4) *Training Details*: We mostly followed the training parameters used in our previous work [14], which slightly changes original Mask R-CNN [7] (replacing last sigmoid to softmax). RPN hidden channels are 512 (1024 in [7]), and minimum and maximum size of input image is 600 and 1000. We used the same learning rate 0.00125 (same as [7, 14]) per a batch for training both baseline (instance-only model) and joint model. The learning rate was multiplied by the batch size as following [7, 14, 31]. In the following training experiments, we use the same configuration about number of GPUs (=4) and batch per gpu (=1), so total batch size is $4 = 4 \cdot 1$ and learning rate is $0.005 = 4 \cdot 0.00125$.

5) *Result*: With above training configurations, we trained instance-only (baseline) and joint model. For joint model, we changed the scaling hyper parameter for loss balancing between instance l^{ins} and semantic segmentation l^{sem} .

Table I shows the result of training both instance-only (Mask R-CNN with softmax) and joint model with using ResNet50 as the backbone of feature extractor. It shows that the joint learning model surpasses the baseline model

TABLE II: Results with/without data augmentation.

backbone	model	λ	data augmentation	mPQ
ResNet50	joint	0.25	no	32.3
			yes	42.2

TABLE III: Results with different backbone.

backbone	model	λ	mPQ
ResNet50	instance-only	-	41.0
	joint	0.25	42.2
ResNet101	instance-only	-	43.5
	joint	0.25	44.5

the efficiency of joint learning of instance and semantic occlusion segmentation. The different results by changing the loss balancing parameter λ show that the appropriate value of hyper parameter is $\lambda = 0.25$.

In order to validate the effectiveness of data augmentation, we trained the joint model with and without the augmentation. Table II show the results and we can see the data augmentation is fairly effective in this case.

We also trained with different backbone for feature extractor with replacing ResNet50 with ResNet101. The result is shown in Table III and it shows that the joint model outperforms the baseline model with both backbones. Figure 10 shows the visualization of recognition results of joint model with ResNet101 backbone. It shows that the capability of model to segment the occluded regions even for the heavily occluded object: *avery_binder* in Figure 10d.

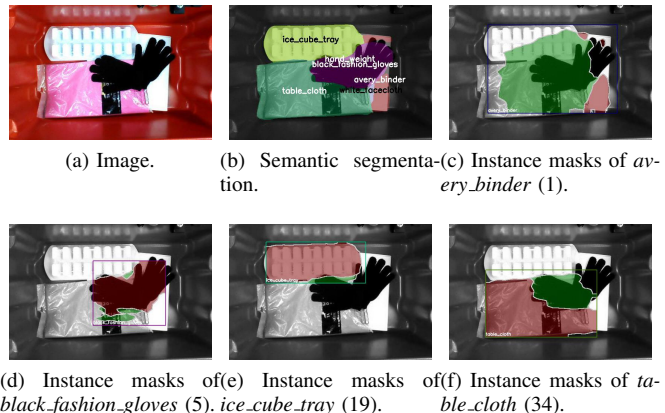


Fig. 10: Qualitative results. The number after object name corresponds to the number in Figure 7. Red mask represents visible, and green mask represents occluded.

B. Robotic Pick-and-Place Experiments

We evaluated the proposed model in the 2 types of robotic pick-and-place tasks:

- Random Picking: in which robot is requested to move all objects from one to another, without any priority of the order.
- Target Picking: in which robot is requested to pick a designated object, with removing the obstacle object appropriately.

Even in the target picking, random picking strategy can be also used, however, picking without any priority takes time to reach to the target object.



Fig. 11: Random picking. The robot is requested to pick and place of all objects located in left bin (source) to the right bin (destination).

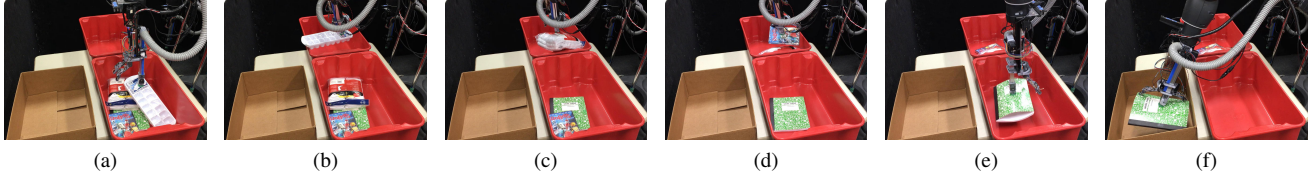


Fig. 12: Target picking. The robot is requested to move a heavily occluded target object (green book) into the cardboard box. Since the target object is occluded by other objects (ice cube tray, socks), the robot needs to detect and remove these obstacle objects into another bin to reach the target object.

1) *Random Picking*: In random picking, there are 2 typical failure cases:

- Next target object is occluded by other heavy objects and can not be picked because of the collision.
- Next target object is occluded by other light objects and robot mistakenly picks 2 or more objects at once.

In general, the former case causes picking failure, time loss and damage to items, and latter case causes dropping one of the picked objects, and wrong count of the picking. To avoid the above problems in random picking, we used occlusion segmentation results to select not-occluded objects as the appropriate next target.

We used 23 objects in Figure 7 which can be graspable by suction for random picking evaluation. The task is moving objects from source (left bin) and destination (right bin) in Figure 11. We used the suction gripper we developed before [32], and used the centroid of point cloud extracted by the visible region segmentation for the suction point.

We randomly created cluttered scenes in the bin, and experimented with the random picking by robot based on the occluded region segmentation. In 67 attempts (1 attempt means picking one object) of pick-and-place, the robot:

- successfully picked an object in 63 times (94.0%);
- failed to grasp because of wrong segmentation of visible regions in 2 times (3%);
- failed to pick because of collision of other object once (1.5%);
- mistakenly picked 2 objects at the same time because of wrong segmentation of occluded regions in once (1.5%).

The result shows the effectiveness of the model to select the fully visible (not-occluded) object in the random picking.

2) *Target Picking*: In target picking, typical failure case is that the target object is so heavily occluded that the robot cannot find it. In this case, the robot can shift to random picking, however, if the target object can be detected even with heavy occlusion, it is useful to plan the appropriate picking order.

Figure 13a shows the typical difficult case of target picking, in which the green book (8 in Figure 7) is located under other 3 objects. Figure 13b, 13c show the visible and occluded mask of each object, in which the same object region is visualized with the same color. Red region represents the masks for the green book, and it shows the model successfully segmented it.

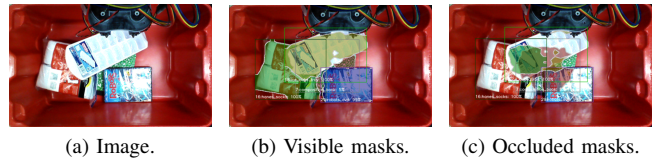


Fig. 13: Typical difficult case of target picking.

Figure 12 shows the demonstration of picking the heavily occluded green book. The bin in closer side is the source location, bin in the further side is the destination for obstacle objects (non target), and the cardboard box is the destination for the target object. This demonstration shows the effectiveness of the model in target picking task with heavily occluded targets.

VI. CONCLUSIONS

We presented the joint learning of instance and semantic segmentation especially for instance-level visible and occluded region segmentation. For collaboration of semantic segmentation with instance occlusion segmentation, we introduced semantic occlusion segmentation extending the conventional semantic visible segmentation. The experimental results showed the effectiveness of the joint training comparing with only training instance segmentation. We also evaluated the model in 2 robotic pick-and-place tasks (random and target picking), and showed the effectiveness in picking tasks of various objects.

REFERENCES

- [1] Jonathan Long, Evan Shelhamer, and Trevor Darrell. Fully Convolutional Networks for Semantic Segmentation. In *Proceedings of the IEEE Conference on Computer Vision and Pattern Recognition (CVPR)*, 2015.
- [2] Liang-Chieh Chieh Chen, George Papandreou, Iasonas Kokkinos, Kevin Murphy, and Alan L. Yuille. DeepLab: Semantic Image Segmentation with Deep Convolutional Nets, Atrous Convolution, and Fully Connected CRFs. *IEEE Transactions on Pattern Analysis and Machine Intelligence (PAMI)*, Vol. 40, No. 4, pp. 834 – 848, 2018.
- [3] Hengshuang Zhao, Jianping Shi, Xiaojuan Qi, Xiaogang Wang, and Jiaya Jia. Pyramid Scene Parsing Network. In *Proceedings of the IEEE Conference on Computer Vision and Pattern Recognition (CVPR)*, 2017.
- [4] Jifeng Dai, Kaiming He, Yi Li, Shaoqing Ren, and Jian Sun. Instance-sensitive Fully Convolutional Networks. In *Proceedings of the European Conference on Computer Vision (ECCV)*, 2016.
- [5] Jifeng Dai, Yi Li, Kaiming He, and Jian Sun. R-FCN: Object Detection via Region-based Fully Convolutional Networks. In *Neural Information Processing Systems (NIPS)*, 2016.
- [6] Yi Li, Haozhi Qi, Jifeng Dai, Xiangyang Ji, and Yichen Wei. Fully Convolutional Instance-aware Semantic Segmentation. In *Proceedings of the IEEE Conference on Computer Vision and Pattern Recognition (CVPR)*, 2016.
- [7] Kaiming He, Georgia Gkioxari, Piotr Dollár, and Ross Girshick. Mask R-CNN. In *Proceedings of the International Conference on Computer Vision (ICCV)*, 2017.
- [8] Rico Jonschkowski, Clemens Eppner, Sebastian Höfer, Roberto Martín-Martín, and Oliver Brock. Probabilistic Multi-Class Segmentation for the Amazon Picking Challenge. In *Proceedings of the IEEE/RSJ Conference on Intelligent Robots and Systems (IROS)*, 2016.
- [9] Kentaro Wada, Kei Okada, and Masayuki Inaba. Probabilistic 3D Multilabel Real-time Mapping for Multi-object Manipulation. In *Proceedings of the IEEE/RSJ Conference on Intelligent Robots and Systems (IROS)*, 2017.
- [10] Andy Zeng, Kuan Ting Yu, Shuran Song, Daniel Suo, Ed Walker, Alberto Rodriguez, and Jianxiong Xiao. Multi-view Self-supervised Deep Learning for 6D Pose Estimation in the Amazon Picking Challenge. In *Proceedings of the IEEE International Conference on Robotics and Automation (ICRA)*, 2017.
- [11] Max Schwarz, Anton Milan, Christian Lenz, Aura Munoz, Arul Selvam Periyasamy, Michael Schreiber, Sebastian Schuller, and Sven Behnke. NimbRo Picking: Versatile Part Handling for Warehouse Automation. In *Proceedings of the IEEE International Conference on Robotics and Automation (ICRA)*, 2017.
- [12] Andy Zeng, Shuran Song, Kuan-Ting Yu, Elliott Donlon, François Hogan, Maria Bauza, Daolin Ma, Orion Taylor, Melody Liu, Eudald Romo, Nima Fazeli, Ferran Alet, Nikhil Chavan Dafle, Rachel Holladay, Isabella Morona, Prem Qu Nair, Druck Green, Ian Taylor, Weber Liu, Thomas Funkhouser, and Alberto Rodriguez. Robotic Pick-and-Place of Novel Objects in Clutter with Multi-Affordance Grasping and Cross-Domain Image Matching. In *Proceedings of the IEEE International Conference on Robotics and Automation (ICRA)*, 2018.
- [13] Max Schwarz, Christian Lenz, Seongyong Koo, Arul Selvam Periyasamy, Michael Schreiber, and Sven Behnke. Fast Object Learning and Dual-arm Coordination for Cluttered Stowing, Picking, and Packing. In *Proceedings of the IEEE International Conference on Robotics and Automation (ICRA)*, 2018.
- [14] Kentaro Wada, Shingo Kitagawa, Kei Okada, and Masayuki Inaba. Instance Segmentation of Visible and Occluded Regions for Finding and Picking Target from a Pile of Objects. In *Proceedings of the IEEE/RSJ Conference on Intelligent Robots and Systems (IROS)*, 2018.
- [15] Pedro O. Pinheiro, Ronan Collobert, Piotr Dollár, and Piotr Dollár. Learning to Segment Object Candidates. In *Neural Information Processing Systems (NIPS)*, 2015.
- [16] Pedro O. Pinheiro, Tsung Yi Lin, Ronan Collobert, and Piotr Dollár. Learning to Refine Object Segments. In *Proceedings of the European Conference on Computer Vision (ECCV)*, 2016.
- [17] Shaoqing Ren, Kaiming He, Ross Girshick, and Jian Sun. Faster R-CNN: Towards Real-Time Object Detection with Region Proposal Networks. In *Neural Information Processing Systems (NIPS)*, 2015.
- [18] Arsalan Mousavian, Hamed Pirsiavash, and Jana Kosecka. Joint Semantic Segmentation and Depth Estimation with Deep Convolutional Networks. In *Proceedings of the International Conference on 3D Vision (3DV)*, 2016.
- [19] Jingchun Cheng, Yi-Hsuan Tsai, Shengjin Wang, and Ming-Hsuan Yang. SegFlow: Joint Learning for Video Object Segmentation and Optical Flow. In *Proceedings of the International Conference on Computer Vision (ICCV)*, 2017.
- [20] Anil S. Baslamisli, Thomas T. Groenestege, Partha Das, Hoang-An Le, Sezer Karaoglu, and Theo Gevers. Joint Learning of Intrinsic Images and Semantic Segmentation. In *Proceedings of the European Conference on Computer Vision (ECCV)*, 2018.
- [21] Kaiming He, Xiangyu Zhang, Shaoqing Ren, and Jian Sun. Deep Residual Learning for Image Recognition. In *Proceedings of the IEEE Conference on Computer Vision and Pattern Recognition (CVPR)*, 2016.
- [22] Jia Deng, Wei Dong, Richard Socher, Li-Jia Li, Kai Li, and Li Fei-Fei. ImageNet: A Large-Scale Hierarchical Image Database. In *Proceedings of the IEEE Conference on Computer Vision and Pattern Recognition (CVPR)*, 2009.
- [23] Ross Girshick. Fast R-CNN. In *Proceedings of the International Conference on Computer Vision (ICCV)*, 2015.
- [24] David Eigen, Christian Puhresch, and Rob Fergus. Depth Map Prediction from a Single Image using a Multi-Scale Deep Network. In *Neural Information Processing Systems (NIPS)*, 2014.
- [25] David Eigen and Rob Fergus. Predicting Depth, Surface Normals and Semantic Labels with a Common Multi-Scale Convolutional Architecture. In *Proceedings of the International Conference on Computer Vision (ICCV)*, 2015.
- [26] Andy Zeng, Shuran Song, Stefan Welker, Johnny Lee, Alberto Rodriguez, and Thomas Funkhouser. Learning Synergies between Pushing and Grasping with Self-supervised Deep Reinforcement Learning. In *Proceedings of the IEEE/RSJ Conference on Intelligent Robots and Systems (IROS)*, 2018.
- [27] Shun Hasegawa, Kentaro Wada, Kei Okada, and Masayuki Inaba. Detecting and Picking of Folded Objects with a Multiple Sensor Integrated Robot Hand. In *Proceedings of the IEEE/RSJ Conference on Intelligent Robots and Systems (IROS)*, 2018.
- [28] Alexey Dosovitskiy, Philipp Fischer, Eddy Ilg, Philip Häusser, Caner Hazirbas, Vladimir Golkov, Patrick van der Smagt, Daniel Cremers, and Thomas Brox. FlowNet: Learning Optical Flow with Convolutional Networks. In *Proceedings of the International Conference on Computer Vision (ICCV)*, 2015.
- [29] Karen Simonyan and Andrew Zisserman. Very Deep Convolutional Networks for Large-Scale Image Recognition. In *Proceedings of the International Conference on Learning Representations (ICLR)*, 2015.
- [30] Alexander Kirillov, Kaiming He, Ross Girshick, Carsten Rother, and Piotr Dollár. Panoptic Segmentation. *arXiv preprint arxiv:1801.00868*, 2018.
- [31] Priya Goyal, Piotr Dollár, Ross Girshick, Pieter Noordhuis, Lukasz Wesolowski, Aapo Kyrola, Andrew Tulloch, Yangqing Jia, and Kaiming He. Accurate, Large Minibatch SGD: Training ImageNet in 1 Hour. *arXiv preprint arxiv:1706.02677*, 2017.
- [32] Shun Hasegawa, Kentaro Wada, Yusuke Niitani, Kei Okada, and Masayuki Inaba. A Three-Fingered Hand with a Suction Gripping System for Picking Various Objects in Cluttered Narrow Space. In *Proceedings of the IEEE/RSJ Conference on Intelligent Robots and Systems (IROS)*, 2017.